



HAL
open science

Physiological transition of *Chlorella vulgaris* from planktonic to immobilized conditions

Sufang Li, Andrea Fanesi, Thierry Martin, Filipa Lopes

► **To cite this version:**

Sufang Li, Andrea Fanesi, Thierry Martin, Filipa Lopes. Physiological transition of *Chlorella vulgaris* from planktonic to immobilized conditions. *Algal Research - Biomass, Biofuels and Bioproducts*, 2024, 77, pp.103354. 10.1016/j.algal.2023.103354 . hal-04404723

HAL Id: hal-04404723

<https://hal.science/hal-04404723>

Submitted on 19 Jan 2024

HAL is a multi-disciplinary open access archive for the deposit and dissemination of scientific research documents, whether they are published or not. The documents may come from teaching and research institutions in France or abroad, or from public or private research centers.

L'archive ouverte pluridisciplinaire **HAL**, est destinée au dépôt et à la diffusion de documents scientifiques de niveau recherche, publiés ou non, émanant des établissements d'enseignement et de recherche français ou étrangers, des laboratoires publics ou privés.

1 **Physiological transition of *Chlorella vulgaris* from planktonic to immobilized**
2 **conditions**

3
4 **Sufang Li, Andrea Fanesi, Thierry Martin, Filipa Lopes***

5 *Laboratoire Génie des Procédés et Matériaux (LGPM), CentraleSupélec, Université Paris-Saclay, 91190 Gif-sur-*
6 *Yvette, France*

7 ** Corresponding author*

8 *E-mail address: filipa.lopes@centralesupelec.fr*

9

10 **ABSTRACT**

11

12 Biofilm-based technologies present many advantages (e.g., higher productivity, lower water
13 demand and harvesting costs) compared with the conventional planktonic approaches for
14 microalgae cultivation. A better understanding of photosynthetic biofilm formation is though still
15 needed in order to develop and run biofilm-based systems at large-scale. In this study, for the first
16 time the physiological transition of *C. vulgaris* cells from planktonic to immobilized state was
17 tracked (cell number, morphology, photosynthetic performance, and cellular composition) during
18 the first 24 hours of immobilization. The results clearly confirmed that microalgae rapidly
19 respond to immobilization via physiological adjustments. Over very short time-scales (3 hours),
20 cells used photosynthesis to grow (increase in size, 140%), at expense of cell division, and
21 adjusted their carbon allocation patterns (increase in the relative carbohydrates pool, 135%). The
22 experiments confirmed that this behavior is specific to cells in the immobilized state. Triggering
23 factors such as water and/or nutrient availability may be responsible for this fast acclimation
24 process. Additionally, lipid content doubled by the end of cultivation, possibly due to imbalanced

1 carbon and nitrogen metabolisms. These results offer new insights for understanding the
2 mechanisms involved in microalgae biofilm formation and development, further helping the
3 operators to optimize the biofilm-based systems.

4
5 **Key words:** Acclimation, *Chlorella vulgaris*, Immobilized state, Physiological transition,
6 Planktonic state, Microalgae biofilms

7 8 **1. Introduction**

9
10 The use of biofilm-based technology for microalgae cultivation has recently become a
11 growing field of research due to their advantages in comparison to conventional photobioreactors
12 or raceways. Indeed, the possibility to grow microalgae attached to a substrate reduces the overall
13 water requirements and the energetic expenses related to biomass harvesting and drying, making
14 the cultivation process more cost-effective. Nevertheless, their use at the commercial scale is still
15 limited. Understanding the mechanisms of biofilm development and physiological adjustments
16 during the cultivation phases will certainly help establishing standard operative procedures, and
17 ultimately setting up this emergent technology at large scale.

18 At present, most of the knowledge we have about physiological responses to external
19 perturbations in microalgae comes from the phytoplankton. Typical response mechanisms
20 include, depending on the time scales, regulation (over minutes) which describes the adjustments
21 of catalytic efficiency of enzymes that occurs without net synthesis or breakdown of
22 macromolecules, and acclimation (over hours or days) that involves a whole macromolecular
23 reorganization at the cell level [1,2]. Both strategies have been extensively described for
24 microalgae cultures in suspension [2], however these mechanisms are poorly studied in biofilm-

1 based systems [3,4]. Indeed, it is possible that the typical acclimation processes described for
2 suspended cultures could not fit when microalgae live in sessile mode, as cells may present
3 different response strategies as a function of their lifestyle [5,6].

4 In biofilms, microalgae cells are enclosed in an extracellular scaffold made of several
5 polymers and water [7,8], and this complex architecture creates a completely different micro-
6 environment from that of their planktonic analogs that are typically surrounded by a less variable
7 environment [6,9]. Gradients of nutrients and light, bulk hydrodynamics or humidity are already
8 known to affect biofilm development [10–13]. Initial adhesion, which may last several hours or
9 days, is a key step affecting biofilm formation [14,15] and dramatic changes in physiological
10 states may occur within this period in which planktonic cells need to rapidly acclimate to the new
11 environmental conditions [16,17]. From a process point of view, the inoculum step (i.e., in
12 biofilms the adhesion of the cells) is of paramount importance to ensure healthy and productive
13 biofilms.

14 Up to date, information regarding the cellular adjustments occurring during a transition from
15 the planktonic state to biofilm have been reported only for bacteria [18,19]. Some works tried to
16 decipher the driving force behind the lifestyle transition from the perspective of molecular
17 pathways, like the expression of biofilm-associated genes or proteins [19,20]. In a previous study
18 [21], the authors listed a battery of genes implicated in cell motility, adhesion and quorum
19 sensing that are essential players in biofilm formation. Also, phenotypic changes in e.g. cell
20 morphology, cell surface structures and organelles (such as flagella, pili and appendages)
21 participating in the biofilm formation were also observed from free-living to surface-attached
22 cells [22–24]. It should be stressed that planktonic microalgae can rapidly (i.e., from minutes to
23 hours) acclimate to shifts in nutrients and light levels [17,25]. We therefore cannot rule out a
24 physiological transition in microalgae from planktonic to biofilm like that occurring in bacteria.

1 To the best of our knowledge, only one study on microalgae has characterized the metabolic
2 differences between planktonic cells and those in a mature biofilms [26]. However, information
3 regarding how microalgae tune their physiological state to acclimate during a shift from
4 planktonic to immobilized conditions has never been studied before.

5 The present work aimed at characterizing the physiological behavior of microalgae when
6 shifting from planktonic to immobilized states. In order to do that, we immobilized *C. vulgaris* on
7 filter membranes to track the physiological adjustments including growth, morphology (cell size),
8 photosynthetic performance and macromolecular composition in the first 24 hours after
9 immobilization. This study may give a basis and new insight for understanding the transition of
10 microalgae from planktonic to benthic lifestyle. From a practical point of view, it may help
11 optimizing microalgae biofilm-based technologies for biomass and/or compounds production by
12 identifying eventual stress factors during the early phases of biofilm formation.

13

14 **2. Materials and Methods**

15

16 *2.1. Inoculum - Planktonic culture maintenance*

17

18 Planktonic cultures of *Chlorella vulgaris* SAG 211–11b (Göttingen, Germany) were grown
19 semi-continuously in a 1 L transparent bottle with 800 mL 3N-Bristol medium at an average
20 irradiance of 250 $\mu\text{mol photons m}^{-2} \text{ s}^{-1}$ (50W LED, the irradiance was measured inside the bottles
21 by a QSL-2100 quantum scalar irradiance sensor, Biospherical Instruments, San Diego, CA,
22 USA) at 25°C. The cultures were bubbled with filtered air and maintained within a range of
23 chlorophyll *a* (Chl *a*) concentration from 0.25 to 1.0 mg L⁻¹ by daily dilution. The planktonic
24 cultures were pre-acclimated to the growth condition for at least 8 days before starting any

1 experiment (after acclimation, the specific growth rate, μ , of the culture was calculated based on
2 cell number ($\mu = 1.4 \pm 0.24 \text{ d}^{-1}$).

3

4 *2.2. Immobilized growth of C. vulgaris on filter membranes*

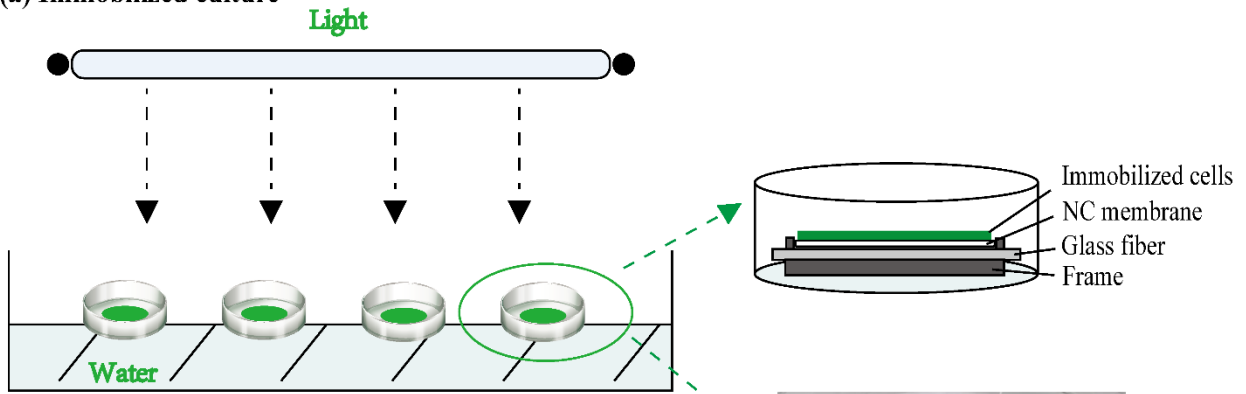
5

6 Immobilized cells of *C. vulgaris* were cultured in the system reported in Fig. 1a [27]. The
7 planktonic cells from the inoculum culture (section 2.1) were gently vacuum-filtered on nitrate
8 cellulose filters (NC) (25-mm diameter, 0.2 μm pore size, Whatman, the effective colonization
9 area was 2.01 cm^2) with an initial cell density of $(27.0 \pm 1.1) \times 10^6 \text{ cells cm}^{-2}$. Membranes were
10 then placed on the glass fiber filters (working as an absorbing material for the medium; 0.2 μm
11 pore size, 47-mm diameter, Whatman) and illuminated at $250 \mu\text{mol photons m}^{-2} \text{ s}^{-1}$ (same light
12 intensity used for the planktonic inoculum, LI-190R Quantum Sensor, LI-COR Biosciences
13 GmbH, Bad Homburg, Germany). Filters were then placed in sterile petri dishes (55-mm
14 diameter) filled with 3 mL of 3N-Bristol medium.

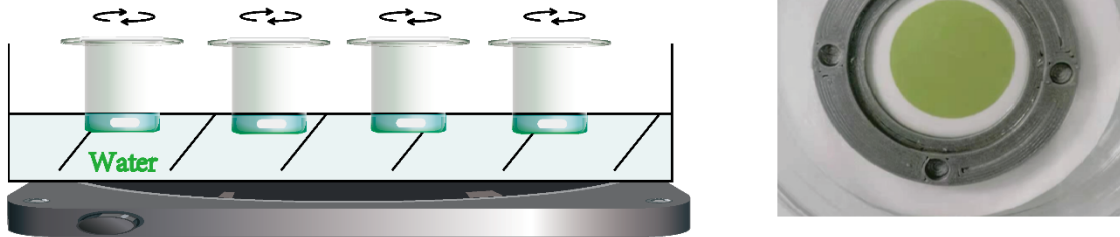
15 After immobilization, the cells were harvested after 1h, 3h, 6h and 24h, respectively. Time 0 h
16 correspond to data of the planktonic culture (inoculum). Physiological measurements of the
17 filtered cells just after immobilization were also carried out in order to ensure that the filtration
18 had no effect on cell physiology. Measurements were conducted immediately after sample
19 collection at each time point to characterize a series of physiological parameters.

20

(a) Immobilized culture



(b) Suspended culture



1

2 **Fig 1.** Schematic representation of the cultivation systems used for the immobilized (a) and
3 suspended cultures (b) of *C. vulgaris* (NC membrane represents cellulose nitrate membrane filter,
4 and water circulated at 25 °C was used to control temperature).

5

6 2.3. Planktonic versus immobilized cultures

7

8 In order to compare the behavior of suspended and immobilized cells, suspended cultures (Fig.
9 1b) with the same number of pre-acclimated cells as those filtrated on the membranes were
10 grown in small glass beakers (25 mL) with 3 mL Bristol medium (around 3.6 mm water depth).
11 The cultures were mixed with a magnetic stirrer and exposed to $250 \mu\text{mol photons m}^{-2} \text{s}^{-1}$ at 25°C
12 as the immobilized cells.

13

1 2.4. Cell number

2

3 Cell number of planktonic and immobilized cultures were measured through flow cytometry
4 (Guava EasyCyte HT; Millipore, USA). For the immobilized cultures, the cells were recovered in
5 two steps. First, the membranes were rinsed with fresh medium (3N-Bristol). This allowed to
6 harvest most of the cells from the support. Second, the membranes with the remaining cells were
7 placed in 50 mL centrifuge tubes and vortexed with fresh medium for 10 seconds. After
8 vortexing, suspensions from both steps were combined to determine total cell numbers by
9 cytometry, as described in [28]. Algal solutions were diluted to a cell concentration range of (1.0
10 – 6.0) $\times 10^5$ cells mL^{-1} before the measurement. Cells were detected by chlorophyll *a*
11 fluorescence (excitation at 488 nm and detection at 680 nm). In planktonic cultures cell numbers
12 were expressed as cell mL^{-1} , whereas in immobilized state the cell areal density (cells cm^{-2}) on
13 the membrane was calculated based on the effective colonization area (2.01 cm^{-2} = the effective
14 filtration area).

15

16 2.5. Cell volume

17

18 Cell morphological changes were observed with an AxioSkop 2 plus microscope (Carl Zeiss,
19 Oberkochen, Germany) using a 63 \times magnification lens. Average volumetric cell size was
20 determined considering a minimum of 300 individual cells by AxioVision SE64 Rel. 4.9.1
21 Software (Zeiss, White Plains, NY, USA) [29].

22

23 2.6. Photosynthetic performance

1
2 Photosynthetic activity was assessed with a Pulse amplitude modulation (PAM) fluorometer
3 (AquaPen, AP 110-C, Photon Systems Instruments, Drasov, Czech Republic). After 10 min of
4 dark-incubation, the samples were exposed to a stepwise increase of seven actinic lights (from 0
5 to 1000 $\mu\text{mol photons m}^{-2} \text{s}^{-1}$, blue led at 455 nm) with 60s intervals to construct the electron
6 transport rate versus photon flux density (ETR/PFD) curves. The relative electron transport rate
7 (rETR) was calculated as described in [30], and the rETR/PFD curves were fitted with the
8 function $r\text{ETR} = r\text{ETR}_{\text{max}} (1 - e^{-\alpha I/r\text{ETR}_{\text{max}}})$ [31] to estimate the maximum rETR ($r\text{ETR}_{\text{max}}$), the
9 initial slope of curves α and photo-saturation irradiance E_k ($E_k = r\text{ETR}_{\text{max}}/\alpha$).

10

11 2.7. Cell components: Chlorophyll *a*, macromolecular and elemental composition

12

13 Chl *a* was extracted with dimethyl sulfoxide (DMSO) [27,32]. Approximately 1.5×10^7 cells
14 were collected by centrifugation and then incubated with 1 mL DMSO at 65 °C for 60 min. The
15 absorbance at 649 nm and 665 nm were measured using an Evolution 60S UV–visible
16 spectrophotometer (Thermo Scientific, Madison, WI, USA). The chl *a* concentration ($\mu\text{g mL}^{-1}$)
17 was quantified using the equation described by [27,32] and the Chl *a* content on a per-cell-
18 volume basis ($\text{fg } \mu\text{m}^{-3}$) was then calculated.

19 ATR-FTIR PerkinElmer Spectrum-two spectrometer (PerkinElmer, Waltham, MA, USA) was
20 used to track variations in cells macromolecules as described by Fanesi et al. [7]. The spectra
21 were baselined and the relative size of the macromolecular pools was characterized based on the
22 maximum absorption values at the corresponding spectral ranges: carbohydrates (C–O–C; 1200–
23 950 cm^{-1}), lipids (C=O; $1750\text{--}1700 \text{ cm}^{-1}$), proteins (Amide I; $1700\text{--}1630 \text{ cm}^{-1}$).

1 The ratio of carbon (C) to nitrogen (N) at 0h and 24h was measured with an elemental analyzer
2 (Organic Elemental Analyzer FLASH 2000 CHNS/O, Thermo Scientific). Dried biomass (1~2
3 mg) harvested from immobilized cultures was used for the analysis after being previously washed
4 twice with MilliQ water and dried at 100°C until a constant weight was reached. Carbon and
5 nitrogen quotas were expressed per cell volume.

6

7 *2.8. Light measurements in the biofilm and suspended culture*

8

9 Light intensity at the bottom of the biofilms was estimated according to the Lambert-Beer
10 model [33]:

11

$$12 \quad I_{bottom} = I_0 e^{-hb} \quad (1)$$

13

14 Where I_{bottom} ($\mu\text{mol photons m}^{-2} \text{ s}^{-1}$) corresponds to the light intensity in the deepest layer of
15 the biofilm (in contact with the support), I_0 stands for the incident light ($= 250 \mu\text{mol photons m}^{-2}$
16 s^{-1}), h is the biofilm thickness at time 0 ($51.2 \pm 10.4 \mu\text{m}$, [27]) and b corresponds to the biofilm
17 extinction coefficient ($5.5 \times 10^3 \text{ m}^{-1}$, [33]).

18 In order to calculate the average irradiance received by the microalgae in the suspended
19 culture (see section 2.3), one defined optical depth λ which reflects the actual amount of light
20 absorbed was calculated using Eq (2) [34]:

21

$$22 \quad \lambda = \xi z = \ln(I_0 / I_z) \quad (2)$$

23

1 Where ξ is the light absorption coefficient and I_z is the light intensity at the depth of z
2 (distance from the illuminating surface, here $z = 3.6$ mm). According to the incident and
3 transmitted light (at bottom of the beaker) intensities measured using the quantum sensor, the
4 value of λ is 0.2033. Thus, assuming that the algal cultures were homogeneous, the average
5 irradiance (I_{av}) received by cells across the cultures could be calculated by Eq (3) [34]:

$$7 \quad I_{av} = I_0/z * \int_0^z \exp(-\xi z) dz = I_0/\lambda * [1 - \exp(-\lambda)] \quad (3)$$

8

9 *2.9. Relative air humidity for immobilized culture*

10

11 To monitor the changes in relative air humidity to which the immobilized cells were exposed,
12 a humidity sensor (P750, Dostmann) was placed inside the Petri dishes. The growth chamber was
13 immediately covered with the lid following the algal immobilization, and the humidity was
14 recorded during the 24 hours of incubation.

15

16 *2.10. Statistics*

17

18 All experiments were performed on three independent biological replicates and the data are
19 reported as mean values with standard deviations (SD). In order to explore the physiological
20 transition of microalgae during the transition from planktonic to immobilized state over time, a
21 principal component analysis (PCA) and a heatmap were computed using R software [35]
22 (combined with packages Vegan and NMF), respectively. The cell areal density, average cell bio-
23 volume, and physiological transitions in photosynthetic parameters and biochemical composition

1 over time were statistically analyzed by one-way ANOVA using IBM SPSS Statistics 25.0
2 software (SPSS Inc., Chicago, IL). Scheffe's multiple comparisons procedure was carried out
3 after the tests of normality and variance homogeneity. Student's *t*-test was employed to test for
4 differences between C (or N) quotas of pre-acclimated planktonic and immobilized cells at end of
5 the cultivation. Significant differences at a level of $P < 0.05$ are shown with different letters.

6

7 **3. Results and discussion**

8

9 *3.1. Physiological transition from planktonic to immobilized state*

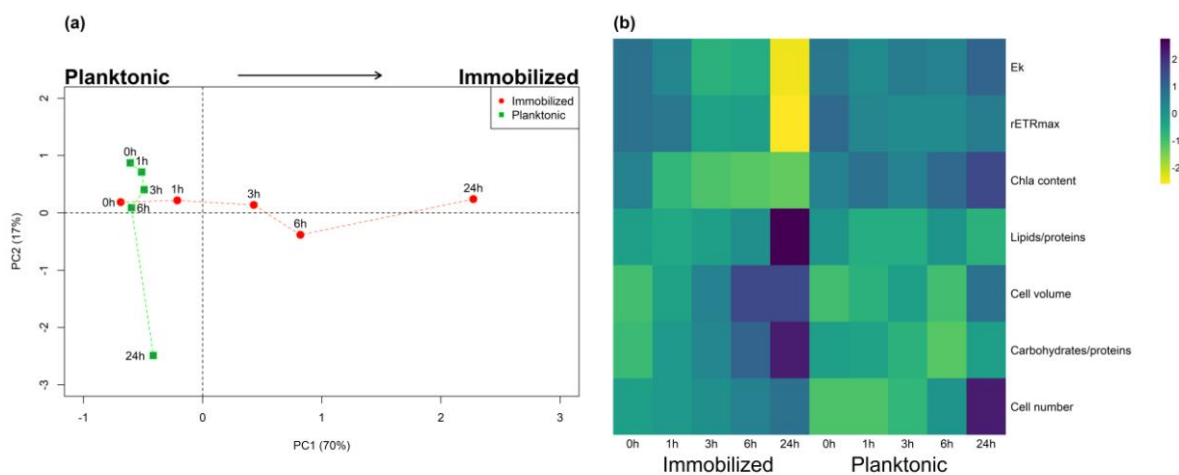
10

11 Environmental conditions (light, nutrients, temperature, etc.) may change rapidly on time
12 scales that match those of cellular processes in aquatic ecosystems [36]. Besides regulation and
13 adaptation, acclimation is the main strategy utilized by photosynthetic organisms to cope with
14 such changes [2]. As an example, variations in pigment synthesis or breakdown in marine
15 phytoplankton have been described due to photo-acclimation that occurs on timescales typical of
16 water mixing in the open ocean, and rapid changes in activity of different components of the
17 photosynthetic apparatus were observed in estuaries [36]. These mechanisms are thought to act
18 according to the main rule of optimizing the balance between light energy absorption and the
19 overall photosynthetic capacity of a cell to protect from excess energy and to finally maximize
20 growth. Extensive research on the subject has been performed on planktonic cultures [17,37,38]
21 and on complex microphytobenthic communities [39–41] or in general on mature natural
22 biofilms [42]. However, no information concerning how microalgae acclimate during the first

1 stages of substrate colonization exists, even though this knowledge could help understanding how
2 microalgae biofilms form, develop and in turn to optimize culture production.

3 For the first time, our results revealed that in *C. vulgaris* the transition from planktonic to
4 immobilized state triggered very fast changes in the cells (Fig. 2). The PCA (Fig. 2a) clearly
5 shows a gradual separation of the samples along the PC1 (70% of variance explained) on the base
6 of their physiological changes over time. Interestingly, such a separation was evident only for the
7 cells that were immobilized, whereas the cells in the planktonic state did not show remarkable
8 physiological adjustments over the first hours (0 - 6h), and the separation after 24h along the PC2
9 (17% of variance explained) was mainly due to an increase in cell number (Fig. 2b, Table S1).
10 These results confirm that the short-term physiological changes were biofilm-specific. Our results
11 are in agreement with other studies that report differences between planktonic and immobilized
12 cultures [6,10]. For instance, it has been demonstrated that cells immobilized on surfaces may be
13 less prone to self-shading [10] and more vulnerable to dehydration [13,43]. A higher availability
14 to CO₂ compared to suspended counterparts may be also improved by the direct exposure to gas
15 [10,13,44].

16
17

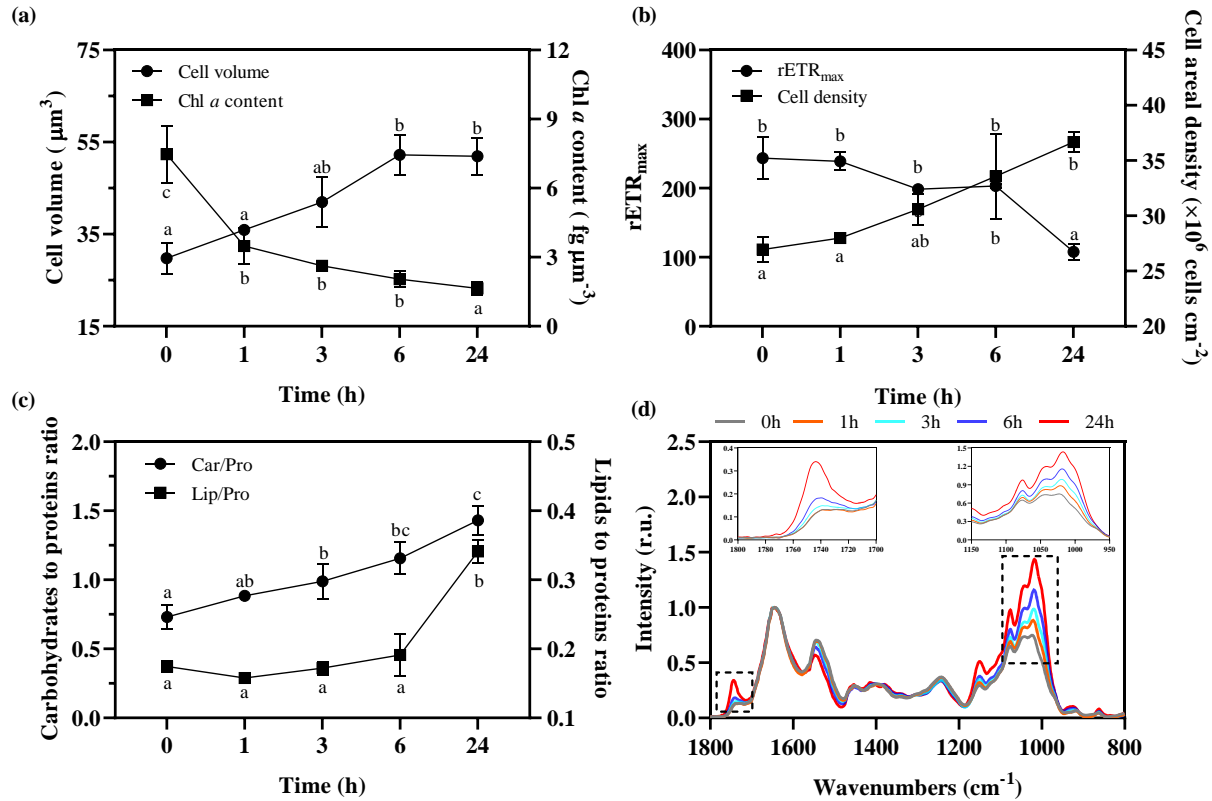


18

1 **Fig. 2.** Scores plot of PCA (a) and heatmap (b) depicting the differences between planktonic and
2 immobilized cells and the patterns of the physiological parameters during the transition (24
3 hours), respectively. In the heatmap, yellow color represents a low value for a specific parameter,
4 whereas dark blue color represents a high value for that parameter.

5
6 In Fig. 2b, the heatmap summarizes the changes in the physiological profile of the cells in the
7 planktonic and in the immobilized states, showing gradual adjustments (from pale green to
8 yellow or to dark blue) of photosynthetic parameters and macromolecules over time. Overall, the
9 cells reacted to the immobilization with an immediate (at 3 or 6 hours) increase in cell volume
10 (140%, Fig. 3a) and relative pool size of carbohydrates (135%, Fig. 3c and 3d), together with a
11 decrease in Chl *a* content per unit volume (already after 1 hour; Fig. 3a). Interestingly, no cell
12 division was observed before 3h from the immobilized state (Fig. 3b). The decrease in the Chl *a*
13 concentration (65%, Fig. 3a) was therefore linked to the increase in cell volume. This is a typical
14 response of cells growing in an unbalanced state when one or more resources are limited [17,38].
15 While photosynthesis was not inhibited ($rETR_{max}$, Fig. 3b), the cells promptly tried to re-balance
16 the absorbed to consumed energy ratio by diluting the Chl *a* content (through the increase in
17 volume) and by accumulating carbohydrates (as a C and electron sink), respectively. Such
18 temporal scales for physiological adjustments have never been described during a transition from
19 planktonic to immobilized states.

20



1
2
3 **Fig. 3.** Changes in average cell volume and Chl *a* quota (a), maximal relative electron transport
4 rate and cell areal density (b), relative carbohydrates and lipids content (c) and FTIR spectra (d)
5 after cells immobilization. The spectra were presented as the average of measurements and
6 normalized by Amide I band (1649 cm^{-1}) which was selected as an internal reference to assess
7 the relative lipids and carbohydrates contents. The peaks corresponding to main organic
8 substances were marked as: carbohydrates (C–O–C; $1174 - 980 \text{ cm}^{-1}$), lipids (C=O; 1737 cm^{-1}),
9 proteins (Amide I; 1649 cm^{-1}), ν = stretching, δ = bending vibrational modes in infrared
10 spectroscopy. All the results were shown as mean value \pm SD ($n = 3$). Bars with different letters
11 represent the statistical differences at level of $P < 0.05$.

12

1 Microalgae (both planktonic and benthonic) are well known to rapidly tune physiological
2 adjustments in response to external cues [25,42,45]. For the phytoplankton, several works
3 reported rapid physiological adjustments to cope with shifts in environmental conditions
4 [25,38,46]. For example, planktonic cells of *Phaeodactylum tricornutum* subjected to a shift in
5 light spectral quality (from blue to red light, or vice versa) exhibited changes in Chl *a* quota,
6 effective quantum yield and cell macromolecules already after 2 hours from the shifts [17]. On
7 the other hand, studies that tracked the physiological changes and biochemical pathways of
8 bacteria during planktonic-to-biofilm transition also confirmed the specific biofilm-related genes
9 or proteins, which were only expressed in benthic but not planktonic bacterial cells [22,47–
10 49,49]. Similarly, natural algal biofilms can rapidly adjust their metabolisms (from minutes to
11 hours) in response to emersion, stressful light conditions, altered humidity and temperature
12 [40,41,50,51]. For instance, Corcoll et al. [52] showed rapid changes (within 6h) in
13 photosynthetic processes of fluvial biofilms after a sudden increase or decrease in the incoming
14 light.

15 In our case, the shift in external conditions related to the immobilized state was hypothesized
16 to have stimulated the physiological response.

17

18 3.2. Factors inducing the transition from planktonic to biofilm state

19

20 Three main factors that could have induced these fast responses after immobilization are
21 proposed: light, humidity and nutrients. While cells in suspended cultures are subjected to
22 dynamic light patterns due to mixing [34,53], in an immobilized system, a light gradient may
23 establish between the top and the bottom of the biofilm and on a short-time scale each biofilm
24 layer is constantly exposed to the same light intensity. Based on our computations, the average

1 light intensity in the immobilized and in the planktonic state was very similar (*ca.* 220 μmol
 2 photons $\text{m}^{-2} \text{s}^{-1}$, Table 1) suggesting that the physiology of the immobilized cells was affected by
 3 other factors. After immobilization, the relative water content (in the gas space of the reactor) for
 4 cells rapidly decreased from 100% in the planktonic solution to 93.5% in the immobilized stage
 5 (Table 1). As demonstrated by Häubner et al. [50] and Shiratake et al. [13], the relative air
 6 humidity affected the photosynthetic activity, chemical composition and growth profiles of
 7 microalgae biofilms. In a water-saturated atmosphere (100% air humidity), cells presented a high
 8 growth profile and photosynthetic efficiency, while at humidity of around 93%, they were
 9 strongly inhibited [50].

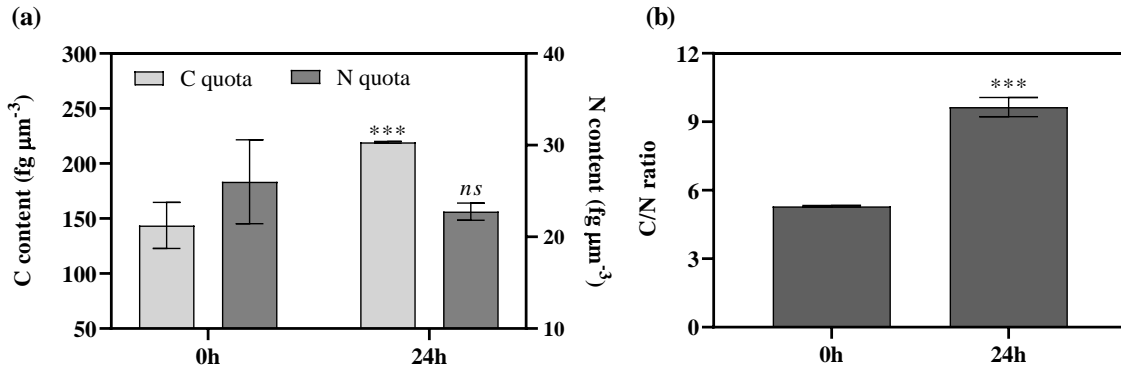
10

11 **Table 1.** Light profiles and relative air humidity of planktonic and immobilized cultures.

Cultures	I_0 ($\mu\text{mol photons m}^{-2} \text{s}^{-1}$)	I_{bottom} ($\mu\text{mol photons m}^{-2} \text{s}^{-1}$)	I_{av} ($\mu\text{mol photons m}^{-2} \text{s}^{-1}$)	Relative air humidity (%)
Planktonic	250	204	226	100
Immobilized	250	189	218	93.5

12

13 Accordingly, although the photosynthetic activity was not affected in the first hours of
 14 immobilization, at 24h a decrease in photosynthetic efficiency ($r\text{ETR}_{\text{max}}$, Fig. 3b) was observed,
 15 together with a 2.0-fold increase in the lipids content in the cells (Fig. 3c and 3d). The latter was
 16 also reflected in a change in cell stoichiometry: while nitrogen quota kept stable, the carbon quota
 17 ($\text{fg } \mu\text{m}^{-3}$; Fig. 4a) significantly increased after 24h resulting in a greater C/N ratio (1.8 folds; Fig.
 18 4b), which suggests an uncoupling between carbon and nitrogen metabolisms.



1
 2 **Fig. 4.** Carbon (or nitrogen) content (a) and C/N ratio (b) in the immobilized cells at the
 3 beginning and end of cultivation. All the results were shown as mean value \pm SD ($n = 3$). Bars
 4 with *** depicts the statistical differences at a level of $P < 0.001$, while *ns* represents no
 5 statistically significant difference.

6
 7 Typically, nutrients may modulate photosynthetic activity in several ways depending on the
 8 limiting compound [54]. The two main ways are the low repairing rate of proteins in
 9 photosystems and the competition for ATP and reducing equivalents between C assimilation and
 10 nutrients uptake [55,56]. On the other hand, a similar trend of $rETR_{max}$ was found by Forster and
 11 Martin-Jézéquel [57] who investigated microphytobenthic diatoms and by Fanesi et al. [58] who
 12 characterized a diatom biofilm. The authors proposed a link between nutrient availability and the
 13 Calvin cycle activity.

14 Interestingly, in another work, a more efficient carbon dioxide mass transfer, and subsequent
 15 productivity, has been suggested in *C. vulgaris* biofilms compared to suspended cultures [10].
 16 Changes in CO₂ concentration could therefore have triggered the physiological transition
 17 observed in the current study. Further experiments are required to deeply investigate the
 18 relationship between photosynthesis and nutrients uptake in photosynthetic biofilms.

1 On the base of these results, it is likely that humidity and nutrients played a major role in the
2 transition from planktonic to immobilized that the cells exhibited.

3 On the whole, the data show that the rapid morphological and physiological changes are
4 specific to the immobilized state. In addition, it is likely that changes in environmental conditions
5 triggered those physiological changes. The rapid acclimation process that the cells underwent
6 immediately after being immobilized seemed to be aimed at optimizing fitness under the new
7 growth conditions [59–61]. Such a great physiological plasticity of cells growing in biofilms, as
8 proposed by other authors, is a key trait to cope with the external variabilities as the biofilm
9 develops [51,57].

10 Further work should be carried out to identify more in detail the underlying acclimation
11 mechanisms and the triggering factors. For instance, a full description of the pigment contents,
12 rates of photosynthesis/respiration, nutrients levels (nitrogen and CO₂) and enzyme activity
13 would certainly allow to assess the underlying biological mechanisms. Furthermore, with the
14 developments in genomics- and proteomics-based approaches, molecular mechanisms/pathways
15 regulating such an acclimation process (from planktonic to immobilized state, or vice versa)
16 could be in future elucidated [19,21].

17

18 **4. Conclusion**

19

20 This study for the first time tracked the physiological behavior of cultured microalgae from
21 planktonic to immobilized condition. The results pointed out that cells rapidly acclimated to the
22 new environmental conditions (surface-associated) by increasing the cell size and adjusting the
23 carbon allocation (carbohydrates pool) (within 6h). Moreover, this behavior seems to be specific
24 of the immobilized state of the cells. We also hypothesized that changes in the local

1 environmental conditions to which cells are exposed might have been responsible for the
2 described cellular behaviors. However, further assays are required to fully comprehend the
3 behavior of cells switching from planktonic to benthic modes. This will represent a step forward
4 to better understand biofilm communities, for the selection of suitable strains and optimize
5 biofilm-based systems.

6

7 **CRedit authorship contribution statement**

8 S. Li: Conceptualization, Investigation, Visualization, Formal analysis, Writing – original draft,
9 Funding acquisition. T. Martin: Conceptualization, Materials fabrication. A. Fanesi:
10 Conceptualization, Investigation, Formal analysis, Writing – review & editing, Funding
11 acquisition. F. Lopes: Supervision, Conceptualization, Formal analysis, Validation, Writing –
12 review & editing.

13

14 **Declaration of competing interest**

15 The authors declare that there is no conflict of interests regarding the publication of this paper.

16

17 **Acknowledgments**

18 S. Li was supported by the China Scholarship Council (CSC) and A. Fanesi was founded from
19 the LabeX LaSIPS project Greenbelt managed by the French National Research Agency (ANR).

20

21 **Data availability**

22 Data will be made available on request.

23

24 **References:**

- 1
- 2 [1] K.H. Halsey, B.M. Jones, Phytoplankton strategies for photosynthetic energy allocation,
3 Annu. Rev. Mar. Sci. 7 (2015) 265–297. <https://doi.org/10.1146/annurev-marine-010814-015813>.
- 4 [2] J.A. Raven, R.J. Geider, Adaptation, acclimation and regulation in algal photosynthesis,
5 in: Photosynth. Algae, Springer, Dordrecht, 2003: pp. 385–412. https://doi.org/10.1007/978-94-007-1038-2_17.
- 6
- 7 [3] A. Mantzorou, F. Ververidis, Microalgal biofilms: A further step over current microalgal
8 cultivation techniques, Sci. Total Environ. 651 (2019) 3187–3201.
9 <https://doi.org/10.1016/j.scitotenv.2018.09.355>.
- 10 [4] J. Wang, W. Liu, T. Liu, Biofilm based attached cultivation technology for microalgal
11 biorefineries - A review, Bioresour. Technol. 244 (2017) 1245–1253.
12 <https://doi.org/10.1016/j.biortech.2017.05.136>.
- 13 [5] J. Wang, J. Liu, T. Liu, The difference in effective light penetration may explain the
14 superiority in photosynthetic efficiency of attached cultivation over the conventional open pond
15 for microalgae, Biotechnol. Biofuels. 8 (2015) 1–12. <https://doi.org/10.1186/s13068-015-0240-0>.
- 16 [6] L.L. Zhuang, J.H. Wang, H.Y. Hu, Differences between attached and suspended
17 microalgal cells in ssPBR from the perspective of physiological properties, J. Photochem.
18 Photobiol. B. 181 (2018) 164–169. <https://doi.org/10.1016/j.jphotobiol.2018.03.014>.
- 19 [7] A. Fanesi, A. Paule, O. Bernard, R. Briandet, F. Lopes, The architecture of monospecific
20 microalgae biofilms, Microorganisms. 7 (2019) 352.
21 <https://doi.org/10.3390/microorganisms7090352>.
- 22 [8] H.C. Flemming, T.R. Neu, D.J. Wozniak, The eps matrix: the “house of biofilm cells,” J.
23 Bacteriol. 189 (2007) 7945–7947. <https://doi.org/10.1128/JB.00858-07>.
- 24 [9] A.E. Toninelli, J. Wang, M. Liu, H. Wu, T. Liu, *Scenedesmus dimorphus* biofilm:
25 Photoefficiency and biomass production under intermittent lighting, Sci. Rep. 6 (2016) 32305.
26 <https://doi.org/10.1038/srep32305>.
- 27 [10] Y. Huang, W. Xiong, Q. Liao, Q. Fu, A. Xia, X. Zhu, Y. Sun, Comparison of *Chlorella*
28 *vulgaris* biomass productivity cultivated in biofilm and suspension from the aspect of light
29 transmission and microalgae affinity to carbon dioxide, Bioresour. Technol. 222 (2016) 367–373.
30 <https://doi.org/10.1016/j.biortech.2016.09.099>.
- 31 [11] T.E. Murphy, H. Berberoglu, Flux balancing of light and nutrients in a biofilm
32 photobioreactor for maximizing photosynthetic productivity, Biotechnol. Prog. 30 (2014) 348–
33 359. <https://doi.org/10.1002/btpr.1881>.
- 34 [12] B. Podola, T. Li, M. Melkonian, Porous substrate bioreactors: a paradigm shift in
35 microalgal biotechnology?, Trends Biotechnol. 35 (2017) 121–132.
36 <https://doi.org/10.1016/j.tibtech.2016.06.004>.

- 1 [13] T. Shiratake, A. Sato, A. Minoda, M. Tsuzuki, N. Sato, Air-drying of cells, the novel
2 conditions for stimulated synthesis of triacylglycerol in a green alga, *Chlorella kessleri*, PLoS
3 ONE. 8 (2013) e79630. <https://doi.org/10.1371/journal.pone.0079630>.
- 4 [14] D.A. Carbone, I. Gargano, G. Pinto, A. Natale, A. Pollio, Evaluating microalgal
5 attachment to surfaces: a first approach towards a laboratory integrated assessment, Chem. Eng.
6 Trans. 57 (2017) 73–78. <https://doi.org/10.3303/CET1757013>.
- 7 [15] R. Sekar, V.P. Venugopalan, K.K. Satpathy, K.V.K. Nair, V.N.R. Rao, Laboratory studies
8 on adhesion of microalgae to hard substrates, Springer, Dordrecht, 2004.
- 9 [16] Y. Meng, A. Li, H. Li, Z. Shen, T. Ma, J. Liu, Z. Zhou, Q. Feng, Y. Sun, Effect of
10 membrane blocking on attached cultivation of microalgae, J. Clean. Prod. 284 (2021) 124695.
11 <https://doi.org/10.1016/j.jclepro.2020.124695>.
- 12 [17] A. Jungandreas, B. Schellenberger Costa, T. Jakob, M. von Bergen, S. Baumann, C.
13 Wilhelm, The Acclimation of *Phaeodactylum tricornutum* to blue and red light does not
14 influence the photosynthetic light reaction but strongly disturbs the carbon allocation pattern,
15 PLoS ONE. 9 (2014) e99727. <https://doi.org/10.1371/journal.pone.0099727>.
- 16 [18] S.L. Chua, S.Y.Y. Tan, M.T. Rybtke, Y. Chen, S.A. Rice, S. Kjelleberg, T. Tolker-
17 Nielsen, L. Yang, M. Givskov, Bis-(3'-5')-cyclic dimeric GPM regulates antimicrobial peptide
18 resistance in *Pseudomonas aeruginosa*, Antimicrob. Agents Chemother. 57 (2013) 2066–2075.
19 <https://doi.org/10.1128/AAC.02499-12>.
- 20 [19] S. Qayyum, D. Sharma, D. Bisht, A.U. Khan, Protein translation machinery holds a key
21 for transition of planktonic cells to biofilm state in *Enterococcus faecalis*: A proteomic approach,
22 Biochem. Biophys. Res. Commun. 474 (2016) 652–659.
23 <https://doi.org/10.1016/j.bbrc.2016.04.145>.
- 24 [20] R.D. Waite, A. Papakonstantinou, E. Littler, M.A. Curtis, Transcriptome analysis of
25 *Pseudomonas aeruginosa* growth: comparison of gene expression in planktonic cultures and
26 developing and mature biofilms, J. Bacteriol. 187 (2005) 6571–6576.
27 <https://doi.org/10.1128/JB.187.18.6571-6576.2005>.
- 28 [21] K.K. Jefferson, What drives bacteria to produce a biofilm?, FEMS Microbiol. Lett. 236
29 (2004) 163–173. <https://doi.org/10.1111/j.1574-6968.2004.tb09643.x>.
- 30 [22] G. O'Toole, H.B. Kaplan, R. Kolter, Biofilm formation as microbial development, Annu.
31 Rev. Microbiol. 54 (2000) 49–79. <https://doi.org/10.1146/annurev.micro.54.1.49>.
- 32 [23] L. Kodjikian, C. Burillon, G. Lina, C. Roques, G. Pellon, J. Freney, F.N.R. Renaud,
33 Biofilm formation on intraocular lenses by a clinical strain encoding the *ica* locus: a scanning
34 electron microscopy study, Investig. Ophthalmology Vis. Sci. 44 (2003) 4382–4387.
35 <https://doi.org/10.1167/iovs.03-0185>.

- 1 [24] X. Zhang, Y. Ma, G. Ye, Morphological observation and comparative transcriptomic
2 analysis of *Clostridium perfringens* biofilm and planktonic cells, *Curr. Microbiol.* 75 (2018)
3 1182–1189. <https://doi.org/10.1007/s00284-018-1507-z>.
- 4 [25] A. Sciandra, L. Lazzara, H. Claustre, M. Babin, Responses of growth rate, pigment
5 composition and optical properties of *Cryptomonas* sp. to light and nitrogen stresses, *Mar. Ecol.*
6 *Prog. Ser.* 201 (2000) 107–120. <https://doi.org/10.3354/meps201107>.
- 7 [26] M.J.L. Romeu, D. Domínguez-Pérez, D. Almeida, J. Morais, A. Campos, V. Vasconcelos,
8 F.J.M. Mergulhão, Characterization of planktonic and biofilm cells from two filamentous
9 cyanobacteria using a shotgun proteomic approach, *Biofouling.* 36 (2020) 631–645.
10 <https://doi.org/10.1080/08927014.2020.1795141>.
- 11 [27] S.F. Li, A. Fanesi, T. Martin, F. Lopes, Biomass production and physiology of *Chlorella*
12 *vulgaris* during the early stages of immobilized state are affected by light intensity and inoculum
13 cell density, *Algal Res.* 59 (2021) 102453. <https://doi.org/10.1016/j.algal.2021.102453>.
- 14 [28] A. Fanesi, M. Lavayssière, C. Breton, O. Bernard, R. Briandet, F. Lopes, Shear stress
15 affects the architecture and cohesion of *Chlorella vulgaris* biofilms, *Sci. Rep.* 11 (2021) 1–11.
16 <https://doi.org/10.1038/s41598-021-83523-3>.
- 17 [29] H. Hillebrand, C.D. Durselen, D. Kirschtel, U. Pollinger, T. Zohary, Biovolume
18 calculation for pelagic and benthic microalgae, *J. Phycol.* 35 (1999) 403–424.
19 <https://doi.org/10.1046/j.1529-8817.1999.3520403.x>.
- 20 [30] A. Guzzon, F. Di Pippo, R. Congestri, Wastewater biofilm photosynthesis in
21 photobioreactors, *Microorganisms.* 7 (2019) 252.
22 <https://doi.org/10.3390/microorganisms7080252>.
- 23 [31] W.L. Webb, M. Newton, D. Starr, Carbon dioxide exchange of *Alnus rubra*, *Oecologia.*
24 17 (1974) 281–291. <https://doi.org/10.1007/BF00345747>.
- 25 [32] N. Qiu, X. Wang, F. Zhou, A new method for fast extraction and determination of
26 chlorophylls in natural water, *Z. Für Naturforschung C.* 73 (2018) 77–86.
27 <https://doi.org/10.1515/znc-2017-0157>.
- 28 [33] J. Grenier, H. Bonnefond, F. Lopes, O. Bernard, The impact of light supply to moving
29 photosynthetic biofilms, *Algal Res.* 44 (2019) 101674.
30 <https://doi.org/10.1016/j.algal.2019.101674>.
- 31 [34] O. Bernard, F. Mairet, B. Chachuat, Modelling of microalgae culture systems with
32 applications to control and optimization, in: *Microalgae Biotechnol.*, Springer, Cham, 2015: pp.
33 59–87. https://doi.org/10.1007/10_2014_287.
- 34 [35] R Core Team, R: A language and environment for statistical computing, (2014).
- 35 [36] H.L. MacIntyre, T.M. Kana, R.J. Geider, The effect of water motion on short-term rates
36 of photosynthesis by marine phytoplankton, *Trends Plant Sci.* 5 (2000) 6.

- 1 [37] T. Anning, H.L. MacIntyre, S.M. Pratt, P.J. Sammes, S. Gibb, R.J. Geider,
2 Photoacclimation in the marine diatom *Skeletonema costatum*, *Limnol. Oceanogr.* 45 (2000)
3 1807–1817. <https://doi.org/10.4319/lo.2000.45.8.1807>.
- 4 [38] M. Ritz, J.C. Thomas, A. Spilar, A.L. Etienne, Kinetics of photoacclimation in response
5 to a shift to high light of the red alga *Rhodella violacea* adapted to low irradiance, *Plant Physiol.*
6 123 (2000) 1415–1426. <https://doi.org/10.1104/pp.123.4.1415>.
- 7 [39] J. Mouget, R. Perkins, M. Consalvey, S. Lefebvre, Migration or photoacclimation to
8 prevent high irradiance and UV-B damage in marine microphytobenthic communities, *Aquat.*
9 *Microb. Ecol.* 52 (2008) 223–232. <https://doi.org/10.3354/ame01218>.
- 10 [40] J. Serôdio, J. Ezequiel, A. Barnett, J. Mouget, V. Méléder, M. Laviale, J. Lavaud,
11 Efficiency of photoprotection in microphytobenthos: role of vertical migration and the
12 xanthophyll cycle against photoinhibition, *Aquat. Microb. Ecol.* 67 (2012) 161–175.
13 <https://doi.org/10.3354/ame01591>.
- 14 [41] M.A. van Leeuwe, V. Brotas, M. Consalvey, D. Gillespie, B. Jesus, J. Roggeveld,
15 Photoacclimation in microphytobenthos and the role of xanthophyll pigments, *Eur. J. Phycol.* 43
16 (2008) 123–132.
- 17 [42] U. Karsten, A. Holzinger, Green algae in alpine biological soil crust communities:
18 acclimation strategies against ultraviolet radiation and dehydration, *Biodivers. Conserv.* 23 (2014)
19 1845–1858. <https://doi.org/10.1007/s10531-014-0653-2>.
- 20 [43] T. Naumann, Z. Çebi, B. Podola, M. Melkonian, Growing microalgae as aquaculture
21 feeds on twin-layers: a novel solid-state photobioreactor, *J. Appl. Phycol.* 25 (2013) 1413–1420.
22 <https://doi.org/10.1007/s10811-012-9962-6>.
- 23 [44] L.L. Zhuang, The characteristics and influencing factors of the attached microalgae
24 cultivation: A review, *Renew. Sustain. Energy Rev.* 94 (2018) 1110–1119.
25 <https://doi.org/10.1016/j.rser.2018.06.006>.
- 26 [45] M. Nymark, K.C. Valle, T. Brembu, K. Hancke, P. Winge, K. Andresen, G. Johnsen, A.M.
27 Bones, An integrated analysis of molecular acclimation to high light in the marine diatom
28 *Phaeodactylum tricornutum*, *PLoS ONE.* 4 (2009) e7743.
29 <https://doi.org/10.1371/journal.pone.0007743>.
- 30 [46] T. Fujiki, S. Taguchi, Variability in chlorophyll a specific absorption coefficient in marine
31 phytoplankton as a function of cell size and irradiance, *J. Plankton Res.* 24 (2002) 859–874.
32 <https://doi.org/10.1093/plankt/24.9.859>.
- 33 [47] S.L. Chua, Y. Liu, J.K.H. Yam, Y. Chen, R.M. Vejborg, B.G.C. Tan, S. Kjelleberg, T.
34 Tolker-Nielsen, M. Givskov, L. Yang, Dispersed cells represent a distinct stage in the transition
35 from bacterial biofilm to planktonic lifestyles, *Nat. Commun.* 5 (2014) 1–12.
36 <https://doi.org/10.1038/ncomms5462>.

- 1 [48] R. Zhao, Y. Song, Q. Dai, Y. Kang, J. Pan, L. Zhu, L. Zhang, Y. Wang, X. Shen, A
2 starvation-induced regulator, RovM, acts as a switch for planktonic/biofilm state transition in
3 *Yersinia pseudotuberculosis*, *Sci. Rep.* 7 (2017) 1–13. [https://doi.org/10.1038/s41598-017-](https://doi.org/10.1038/s41598-017-00534-9)
4 00534-9.
- 5 [49] Y. Zou, J. Woo, J. Ahn, Cellular and molecular responses of *Salmonella typhimurium* to
6 antimicrobial-induced stresses during the planktonic-to-biofilm transition: Antimicrobial-induced
7 responses of foodborne pathogens, *Lett. Appl. Microbiol.* 55 (2012) 274–282.
8 <https://doi.org/10.1111/j.1472-765X.2012.03288.x>.
- 9 [50] N. Häubner, R. Schumann, U. Karsten, Aeroterrestrial microalgae growing in biofilms on
10 facades-response to temperature and water stress, *Microb. Ecol.* 51 (2006) 285–293.
11 <https://doi.org/10.1007/s00248-006-9016-1>.
- 12 [51] R. Perkins, G. Underwood, V. Brotas, G. Snow, B. Jesus, L. Ribeiro, Responses of
13 microphytobenthos to light: primary production and carbohydrate allocation over an emersion
14 period, *Mar. Ecol. Prog. Ser.* 223 (2001) 101–112. <https://doi.org/10.3354/meps223101>.
- 15 [52] N. Corcoll, B. Bonet, M. Leira, B. Montuelle, A. Tlili, H. Guasch, Light history
16 influences the response of fluvial biofilms to Zn exposure, *J. Phycol.* 48 (2012) 1411–1423.
17 <https://doi.org/10.1111/j.1529-8817.2012.01223.x>.
- 18 [53] C. Combe, P. Hartmann, S. Rabouille, A. Talec, O. Bernard, A. Sciandra, Long-term
19 adaptive response to high-frequency light signals in the unicellular photosynthetic eukaryote
20 *Dunaliella salina*, *Biotechnol. Bioeng.* 112 (2015) 1111–1121. <https://doi.org/10.1002/bit.25526>.
- 21 [54] D.D. Wykoff, J.P. Davies, A. Melis, A.R. Grossman, The regulation of photosynthetic
22 electron transport during nutrient deprivation in *Chlamydomonas reinhardtii*, *Plant Physiol.* 117
23 (1998) 129–139. <https://doi.org/10.1104/pp.117.1.129>.
- 24 [55] J. Beardall, E. Young, S. Roberts, Approaches for determining phytoplankton nutrient
25 limitation, *Aquat. Sci.* 63 (2001) 44–69. <https://doi.org/10.1007/PL00001344>.
- 26 [56] D.H. Turpin, Effects of inorganic N availability on algal photosynthesis and carbon
27 metabolism, *J. Phycol.* 27 (1991) 14–20.
- 28 [57] R.M. Forster, V. Martin-Jézéquel, Photophysiological variability of microphytobenthic
29 diatoms after growth in different types of culture conditions, *Phycologia.* 44 (2005) 393–402.
30 [https://doi.org/10.2216/0031-8884\(2005\)44\[393:PVOMDA\]2.0.CO;2](https://doi.org/10.2216/0031-8884(2005)44[393:PVOMDA]2.0.CO;2).
- 31 [58] A. Fanesi, T. Martin, C. Breton, O. Bernard, R. Briandet, F. Lopes, The architecture and
32 metabolic traits of monospecific photosynthetic biofilms studied in a custom flow- through
33 system, *Biotechnol. Bioeng.* 119 (2022) 2459–2470. <https://doi.org/10.1002/bit.28147>.
- 34 [59] R. Geider, H. MacIntyre, T. Kana, Dynamic model of phytoplankton growth and
35 acclimation: responses of the balanced growth rate and the chlorophyll *a*:carbon ratio to light,
36 nutrient-limitation and temperature, *Mar. Ecol. Prog. Ser.* 148 (1997) 187–200.
37 <https://doi.org/10.3354/meps148187>.

1 [60] R.J. Geider, C.M. Moore, O.N. Ross, The role of cost–benefit analysis in models of
2 phytoplankton growth and acclimation, *Plant Ecol. Divers.* 2 (2009) 165–178.
3 <https://doi.org/10.1080/17550870903300949>.

4 [61] R.J. Geider, H.L. MacIntyre, T.M. Kana, A dynamic regulatory model of phytoplanktonic
5 acclimation to light, nutrients, and temperature, *Limnol. Oceanogr.* 43 (1998) 679–694.
6 <https://doi.org/10.4319/lo.1998.43.4.0679>.

7